

# UCLA

## UCLA Previously Published Works

### Title

Differential Contributions of Actin and Myosin to the Physical Phenotypes and Invasion of Pancreatic Cancer Cells.

### Permalink

<https://escholarship.org/uc/item/7nk641bq>

### Journal

Cellular and molecular bioengineering, 13(1)

### ISSN

1865-5025

### Authors

Nguyen, Angelyn V  
Trompetto, Brittany  
Tan, Xing Haw Marvin  
[et al.](#)

### Publication Date

2020-02-01

### DOI


10.1007/s12195-019-00603-1

Peer reviewed



Original Article

# Differential Contributions of Actin and Myosin to the Physical Phenotypes and Invasion of Pancreatic Cancer Cells

ANGELYN V. NGUYEN,<sup>1</sup> BRITTANY TROMPETTO,<sup>1</sup> XING HAW MARVIN TAN,<sup>2</sup> MICHAEL B. SCOTT,<sup>1,7,9,10</sup>  
KENNETH HSUEH-HENG HU,<sup>3</sup> ERIC DEEDS,<sup>1,4</sup> MANISH J. BUTTE,<sup>5,6</sup> PEI YU CHIOU,<sup>2,7</sup>  
and AMY C. ROWAT <sup>1,2,8</sup>

<sup>1</sup>Department of Integrative Biology and Physiology, University of California, 610 Charles E Young Dr. East, Los Angeles, CA 90095, USA; <sup>2</sup>Department of Bioengineering, University of California, Los Angeles, USA; <sup>3</sup>Stanford Biophysics, Stanford University, Stanford, USA; <sup>4</sup>Institute for Quantitative and Computational Biology, University of California, Los Angeles, USA; <sup>5</sup>Department of Pediatrics, University of California, Los Angeles, USA; <sup>6</sup>Department of Microbiology, Immunology, and Molecular Genetics, University of California, Los Angeles, USA; <sup>7</sup>Department of Mechanical and Aerospace Engineering, University of California, Los Angeles, USA; <sup>8</sup>Jonsson Comprehensive Cancer Center, University of California, Los Angeles, USA; <sup>9</sup>Department of Radiology, Northwestern University Feinberg School of Medicine, Chicago, USA; and <sup>10</sup>Department of Biomedical Engineering, Northwestern McCormick School of Engineering, Evanston, USA

(Received 1 July 2019; accepted 4 October 2019; published online 31 October 2019)

Associate Editor Partha Roy oversaw the review of this article.

## Abstract

**Introduction**—Metastasis is a fundamentally physical process in which cells deform through narrow gaps and generate forces to invade surrounding tissues. While it is commonly thought that increased cell deformability is an advantage for invading cells, we previously found that more invasive pancreatic ductal adenocarcinoma (PDAC) cells are stiffer than less invasive PDAC cells. Here we investigate potential mechanisms of the simultaneous increase in PDAC cell stiffness and invasion, focusing on the contributions of myosin II, Arp2/3, and formins.

**Method**—We measure cell invasion using a 3D scratch wound invasion assay and cell stiffness using atomic force microscopy (AFM). To determine the effects of actin- and myosin-mediated force generation on cell stiffness and invasion, we treat cells with pharmacologic inhibitors of myosin II (blebbistatin), Arp2/3 (CK-666), and formins (SMIFH2).

**Results**—We find that the activity of myosin II, Arp2/3, and formins all contribute to the stiffness of PDAC cells. Interestingly, we find that the invasion of PDAC cell lines is differentially affected when the activity of myosin II, Arp2/3, or formins is inhibited, suggesting that despite having similar tissue origins, different PDAC cell lines may rely on different mechanisms for invasion.

**Conclusions**—These findings deepen our knowledge of the factors that regulate cancer cell mechanotype and invasion, and incite further studies to develop therapeutics that target

multiple mechanisms of invasion for improved clinical benefit.

**Keywords**—Mechanobiology, Cytoskeleton, Pancreatic ductal adenocarcinoma, Cell stiffness, Arp2/3, Formins, Traction forces, Cell motility.

## INTRODUCTION

Cell physical phenotypes, including deformability, adhesion, and contractility, are critical in cancer cell invasion.<sup>4,108,112</sup> The physical phenotypes of tumor cells may also be implicated in many steps of metastasis: to spread to distant sites, cells are required to invade into the extracellular matrix, intravasate, and extravasate, which all require movement through micron-scale pores smaller than the diameter of a single cell.<sup>42,108</sup> Physical phenotypes of cancer cells, such as deformability and adhesion, are emerging as label-free, complementary biomarkers for cancer diagnosis.<sup>101</sup> Since the proteins and pathways that regulate cell physical phenotypes also contribute to cell invasion,<sup>4,108,112</sup> mechanotransduction,<sup>14,36,40,85,113</sup> and chemoresistance,<sup>104</sup> understanding the molecular mediators of physical phenotypes can provide mechanistic insight into cancer progression and new therapeutic strategies. For example, cellular contractile force generation is mediated by Rho-associated protein

Address correspondence to Amy C. Rowat, Department of Integrative Biology and Physiology, University of California, 610 Charles E Young Dr. East, Los Angeles, CA 90095, USA. Electronic mail: rowat@ucla.edu

kinase (ROCK). Treatment with the ROCK inhibitor Fasudil reduces invasion *in vitro* and metastasis *in vivo*.<sup>115,122</sup> Fasudil also decreases the physical tension within the tumor to increase tumor porosity and improve chemotherapy access.<sup>104</sup> A deeper knowledge of the relationship between cell physical phenotypes and clinically relevant cell behaviors, such as invasion, could enable identification of new therapeutic strategies to improve patient outcomes.

The mechanical phenotype, or mechanotype, of cells is a physical property that includes cellular deformability, which is the ability of cells to resist shape changes in response to physical forces, and cellular contractile forces, or the magnitude of physical forces cells generate. Mechanotype is emerging as an important property of cancer cells that can change during cancer progression and shows strong associations with *in vitro* measurements of cell invasion,<sup>15,25,43,56,61,74,112,116</sup> which reflect the ability of cells to metastasize *in vivo*.<sup>39</sup> A frequently observed trend is that more invasive tumor cells are more deformable, which has been shown across prostate, ovarian, and breast cancer cell lines *in vitro*,<sup>15,25,56,112</sup> as well as tumor cells of human breast biopsies *in situ*.<sup>51,68</sup> Increased deformability enables cells to transit more easily through narrow gaps,<sup>32,81</sup> and may therefore provide a selective advantage in metastasis. Conversely, cells with decreased cellular and nuclear deformability are more likely to occlude narrow gaps<sup>32,81</sup> and tend to exhibit reduced invasion.<sup>18,72,95,112</sup> However, there are examples where more invasive cells are stiffer, including lung cancer cells,<sup>116</sup> pancreatic ductal adenocarcinoma cells (PDAC),<sup>61</sup> and cancer cells with increased beta-adrenergic signaling.<sup>43</sup> Despite multiple examples of stiffer cells being more invasive, it remains poorly understood what factors contribute to the simultaneous increase in cell stiffness and invasion that is observed in some cell types. With a greater understanding of why stiffer cells are more invasive, we could advance mechanotype as a clinical biomarker and gain insights into novel therapeutic targets.

Cells are complex, dynamic materials, and cellular mechanotype is determined by both intrinsic and extrinsic factors. Intrinsic determinants of cell mechanotype include levels of mechanoregulating proteins, such as cytoskeletal actin<sup>8,9</sup> and nuclear lamins,<sup>80,96</sup> as well as the organization of higher order structures formed by these proteins such as actin filaments. Cell mechanotype is also determined by the forces that cells generate in response to extrinsic factors, such as soluble molecules, the mechanical stiffness of the extracellular matrix, and the balance of intra-

cellular tension across cell–matrix structures and focal adhesions.<sup>107,121</sup> The intrinsic and extrinsic factors that determine cell physical properties also mediate cell motility and invasion.<sup>11,30,55,77</sup> For example, actin is a key structural protein that is also crucial in dynamic cellular behaviors, such as the generation of physical forces through the conversion of ATP into mechanical energy. We previously investigated if stiffer PDAC cells are more invasive because they have higher levels of actin.<sup>61</sup> However, we found no significant differences in the levels of beta-actin or filamentous (F-)actin across cell lines with varying stiffness and invasive potential. Another possible origin of the increased stiffness of more invasive cells could be the actin-dependent force generation that can influence both cell stiffness<sup>8,9,26,95</sup> and invasion.<sup>29,37,69</sup> Reducing actomyosin contractility by pharmacologic inhibition of myosin II results in decreased cell migration and invasion,<sup>37,69</sup> as well as decreased stiffness of fibroblasts and ovarian cancer cells.<sup>9,95</sup> The protrusive forces generated by actin polymerization and branching, which are mediated by the Arp2/3 complex and formins, such as diaphanous proteins, are also critical for certain modes of cancer cell invasion. Reducing the activity of Arp2/3 and formins diminishes the formation of structures involved in motility and invasion such as lamellipodia and invadopodia,<sup>31,93,114</sup> and decreases the invasion of head and neck squamous cancer cells.<sup>29</sup> The activity of Arp2/3 and formins also contribute to cancer cell mechanotype.<sup>28</sup> Thus, we hypothesize that actin-mediated force generation, which is largely regulated by the activity of myosin II, Arp2/3, and formins, contributes to the simultaneous increased invasion and stiffness of cancer cells.

Here we test the hypothesis that more invasive cancer cells are stiffer than their less invasive counterparts due to the activity of myosin II, Arp2/3, and formins. We use a panel of PDAC cell lines as a model system, as they have well-defined mechanotypes and invasive potential<sup>61</sup>; this allows us to investigate factors that contribute to stiffer cells being more invasive across cell lines that have similar tissue origin.<sup>17</sup> We measure cell stiffness using atomic force microscopy (AFM) and invasion using a 3D scratch wound invasion assay, with and without pharmacological inhibition of myosin II, Arp2/3, and formin activity. To develop a more integrated knowledge of PDAC cell invasion, we also measure cellular traction forces and the activity of matrix metalloproteinases (MMPs). Our findings reveal that myosin II, Arp2/3, and formins differentially contribute to cell stiffness and invasion in a cell-type dependent manner.

## EXPERIMENTAL METHODS

### *Cell Culture*

Pancreatic ductal adenocarcinoma (PDAC) cell lines (Hs766T, MIA PaCa-2, and PANC-1) are from the American Type Culture Collection (ATCC). Cell lines were authenticated using the Promega powerplex16 System recommended by ATCC within 1 year of these experiments. Cells are cultured at 5% CO<sub>2</sub> and 37 °C in high glucose, L-glutamine Dulbecco's Modified Eagle Medium (DMEM) (Life Technologies) with 10% fetal bovine serum and 1% v/v penicillin–streptomycin (Gemini BioProducts). To inhibit myosin II, Arp2/3, and formins, cells are treated with 20 μM, or 50 μM of blebbistatin, CK-666, and SMIFH2; vehicle control is DMSO-treated (0.5% w/w). For AFM and micropillar experiments, cells are treated with drugs for 30 min prior to measurement. For scratch-wound invasion experiments, cells are treated with drugs for the duration of each experiment starting at  $t = 0$  h. To inhibit matrix metalloproteinases (MMPs), we treat cells for 48 h with 10 or 25 μM GM6001 prior to measurement of MMP activity levels; for 3D invasion assays, cells are treated with GM6001 for the duration of the experiment.

### *Gene Expression and Bioinformatics Analysis*

To analyze gene expression, we use publicly available RNA-seq data for Hs766T, MIA PaCa-2, and PANC-1.<sup>3</sup> Using STAR v.2.4.2a,<sup>19</sup> we align RNA sequence reads to the human reference genome (hg38) with Ensembl v.82 transcriptome annotations. STAR is run with the following parameters: minimum/maximum intron sizes are set to 30 and 500,000; non-canonical, unannotated junctions are removed; maximum tolerated mismatches is set to 10; and the outSAMstrandField intron motif option is enabled. To quantify per sample read abundances we use the Cuffquant command included with Cufflinks v.2.2.1,<sup>100</sup> with fragment bias correction and multiread correction enabled. All other options are set to default. Finally, fragments per kilobase of exon per million fragments mapped (FPKM) are calculated using the Cuffnorm command with default parameters. We use these FPKM values to compare expression levels of genes whose protein products are implicated in regulation of cell mechanical properties.<sup>16,23,54,91,96,118</sup> We compare arbitrary gene expression values across the 3 cell lines.

### *Atomic Force Microscopy (AFM)*

To measure cell stiffness, AFM is performed as previously described<sup>61</sup> using the MFP-3D-BIO system (Asylum Research, Oxford Instruments). Cells are

probed with the “C” tip of an MLCT probe (Bruker), which has a nominal spring constant of 0.01 N/m. The exact spring constant for each probe is calibrated before each experiment by indenting clean glass and the spring constant is calculated by the thermal noise method. Force–distance curves are acquired by indenting the cytoplasmic region of 20 to 30 cells for each cell line and drug treatment. Approach and retract speeds for all experiments are 5 μm/s. The elastic modulus for each cell is determined by fitting force–distance curves to the Hertz–Sneddon model using Asylum Research software. Experiments were carried out at 37 °C.

### *3D Scratch Wound Invasion and Proliferation Assays*

We perform invasion and proliferation assays using the IncuCyte time-lapse imaging system (EssenBio-science). To measure cell invasion through a 3D matrix, we perform scratch wound invasion assays with Matrigel to simulate the ECM. We plate cells in the wells of a 96-well plate at 95% confluency, create a scratch wound (EssenBioscience WoundMaker), overlay the scratch with 8 mg/mL Matrigel (Corning), and acquire phase contrast images every 4 h for 120 h at 5% CO<sub>2</sub> and 37 °C (IncuCyte Zoom). We determine the confluence of cells in the wound area at each time point using quantitative image analysis (Essen Bioscience). Since wound confluence may be influenced by cell proliferation, we also measure percent confluence by sparsely plating cells (20% confluency) and acquiring phase contrast images every 2 h for 120 h. To quantify the number of protrusions at the invasion front, the length of each invasion front is measured using the free hand tool of ImageJ.

### *Cell Rounding Assay*

To determine the timescale of cell rounding, which is an indicator of myosin II activity, we measure the rate of change in projected cell area after trypsinization. We plate cells to 40% confluency in a 60 mm petri dish coated with 100 μg/mL Matrigel (overnight at 37 °C), wash twice with 1X phosphate buffered saline (Corning), and then treat with 1× trypsin–EDTA to induce cell rounding (Gemini BioProducts). To quantify changes in cell shape during rounding, we acquire images every 10 s starting immediately before trypsin–EDTA is added ( $t = 0$  s). We assess cell rounding by measuring cell area at each time point using a custom MatLab (Mathworks) script. To determine the rounding time constant, we fit a bounded exponential growth model to our data since the normalized area grows from the origin and reaches an asymptote. We use the form:

$$NA = NA_f(1 - \exp(-t/\tau)),$$

where  $NA_f$  is the asymptotic normalized area (i.e. the final area),  $t$  is the time in seconds, and  $\tau$  is the time constant.

#### *Micropillar Traction Stress Assay*

To quantify cellular traction stresses, we use a micropillar assay.<sup>99</sup> We fabricate PDMS micropillars as previously described<sup>110</sup> and embed gold micro-disks in the top of each pillar to facilitate darkfield imaging with a 20x objective (NA 0.5). We image 10 regions of the pillar array before cell seeding. After seeding for 20 h, we treat cells with drugs (30 min), and fix the cells with 4% paraformaldehyde for 15 min at 37 °C. To delineate cells, we label the plasma membrane with wheat germ agglutinin (WGA), Alexa Fluor 488 conjugate (Invitrogen). The same 10 regions of the micropillar devices are then imaged using fluorescence microscopy (Zeiss Axiovert A1) equipped with a 20x objective (NA 0.5) to identify pillars occupied by cells, and darkfield microscopy to track the displacement of the gold-tipped pillars. The traction force,  $F$ , exerted by a cell on a single pillar is determined by:

$$F = \frac{4}{3} \pi E \frac{r^4}{L^3} \Delta x,$$

where  $E$  is the elastic modulus of the pillar (2.0 MPa<sup>111</sup>),  $r$  is the radius of the pillar (measured to be 0.875  $\mu\text{m}$ ),  $L$  is the height of the pillar (measured to be 6.5  $\mu\text{m}$ ), and  $\Delta x$  is the horizontal displacement of the pillar between  $t_0$  and  $t_{\text{measured}}$ .

#### *Matrix Metalloproteinase (MMP) Activity Assay*

To measure the activity of MMPs, we use the MMP Activity Assay (Fluorometric—Red, abcam). In brief, we retrieve 90  $\mu\text{L}$  of conditioned media from each well of a 96-well plate, in which cells are at ~30% confluency after 18 h of culture. Media is transferred to the wells of a black-walled, clear-bottom 96-well plate (Greiner BioProducts). Absorbance at 540/590 nm is measured on a Molecular Devices Flexstation at 90 min after the addition of the MMP substrate.

#### *Statistical Analysis*

All data are obtained from at least three independent experiments. For data with normal distributions, we determine statistical significance using a Student's  $t$  test (Excel, Microsoft). For data that exhibit a non-normal distribution, use the Mann–Whitney U test to determine statistical significance (OriginLab).

## RESULTS

To investigate the relationship between cell stiffness, invasion, and the activity of myosin II, Arp2/3, and formins, we use three immortalized PDAC cell lines: Hs766T, MIA PaCa-2, and PANC-1. The MIA PaCa-2 and PANC-1 cell lines have similar founder mutations (*KRAS*, *TP53*, and *CDKN2A*), while the Hs766T cell line has an additional *SMAD4* mutation.<sup>17</sup> We previously determined that across this panel of PDAC cell lines, more invasive cells tend to be stiffer.<sup>61</sup> The Hs766T cells are the stiffest and most invasive of these three cell lines, while the MIA PaCa-2 are the most deformable and least invasive.<sup>61</sup>

#### *Myosin II Activity has Differential Effects on the Invasion of PDAC Cells*

Myosin II is essential for generating forces involved in motility.<sup>59,94</sup> The activity of myosin II also contributes to cell stiffness.<sup>88,95</sup> Therefore, we first investigate the role of myosin II in the increased invasion of stiffer PDAC cells. Analysis of existing RNA-seq expression data<sup>3</sup> reveals higher expression of genes encoding nonmuscle myosin IIA (MYH9) and myosin IIB (MYH10) in Hs766T compared to PANC-1 and MIA PaCa-2 cell lines (Supp. Fig. 1); these findings suggest that Hs766T cells could have increased myosin II activity and thereby generate a larger magnitude of myosin-II dependent forces, which could contribute to their increased invasion.<sup>2,52</sup> To test this hypothesis, we determine the effect of myosin II activity on PDAC cell invasion using a 3D scratch-wound assay overlaid with a Matrigel protein matrix. To reduce the activity of myosin II, we treat cells with blebbistatin, a small molecule that inhibits myosin II activity.<sup>46</sup> For cells treated with the DMSO vehicle control, we observe that invasion varies across PDAC cell lines, from most to least invasive, Hs766T > PANC1 > MiAPaCa-2 (Fig. 1), which is consistent with our previous findings.<sup>61</sup> Interestingly, we find that blebbistatin treatment has cell line-dependent effects on invasion. Both PANC-1 and MIA PaCa-2 show significant, dose-dependent decreases in invasion with increasing concentrations of blebbistatin. For example, at 72 h, MIA PaCa-2 cells show a modest but significant reduction in wound confluence from  $19 \pm 2\%$  for the DMSO control cells to  $11 \pm 1\%$  for cells treated with 50  $\mu\text{M}$  blebbistatin ( $p = 2.1 \times 10^{-4}$ ). PANC-1 cells exhibit a greater reduction in wound confluence at 72 h from  $30 \pm 1\%$  to  $13 \pm 2\%$  with the 50  $\mu\text{M}$  blebbistatin treatment ( $p = 5.9 \times 10^{-10}$ ) (Fig. 1c). Our results showing reduced invasion of MIA PaCa-2 and PANC-1 cells with decreased myosin II activity are consistent with previous observations that treatment with blebbis-

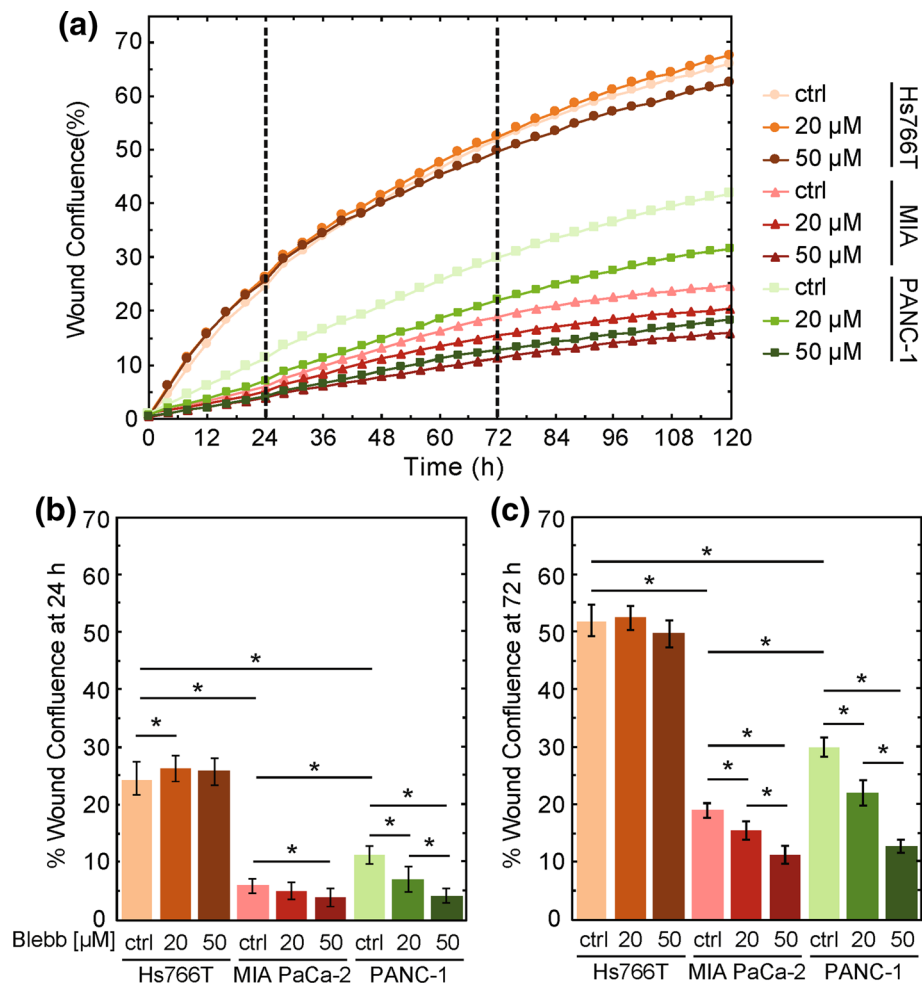


**FIGURE 1.** Myosin II activity is required for the invasion of MIA PaCa-2 and PANC-1 cells, but not Hs766T cells. (a) Invasion through Matrigel is measured by wound confluence in a 3D scratch wound invasion assay. Scatter plot shows the quantification of wound confluence over time. Cells are treated with blebbistatin or DMSO (ctrl) from  $t = 0$ . The dashed lines indicate the 24 h and 72 h time points, which we use to compare wound confluence values for statistical significance. Data points show average invasion over three independent experiments. Bar plot shows average wound confluence at 24 h (b) and 72 h (c). Error bars represent standard error across three independent experiments. Pairwise  $p$  values are determined by a Student's  $t$  test.  $*p < 0.05$ .

tatin<sup>20,37</sup> and ROCK inhibitors<sup>79,103,105</sup> reduces the invasion of cancer cells.<sup>79,103,105</sup> By contrast, Hs766T cells show no significant change in wound confluence with 50 μM blebbistatin treatment when compared to the vehicle control at 72 h ( $50 \pm 2\%$  vs.  $52 \pm 3\%$ ,  $p = 6.1 \times 10^{-1}$ ), suggesting that myosin II activity is not required in the dominant mechanism of invasion of these cells.

Since the invasion measured in this 3D wound confluence assay can be affected by differences in cell proliferation with and without drug treatment, we measure cell proliferation by tracking the confluence of cells over time. While we find some significant changes in proliferation with blebbistatin treatment (Supp. Fig. 2), these observations cannot fully explain the observed differences in invasion. For example, the decrease in the confluence of MIA PaCa-2 cells over time may contribute to their reduced invasion, but the

proliferation of PANC-1 cells is not altered despite their significantly decreased invasion (Fig. 1, Supp. Fig. 2). Thus, differences in cell proliferation across our PDAC cell lines with and without blebbistatin treatment cannot explain the differences we observe in the invasion of these cells when myosin II activity is inhibited. Therefore, our data suggest that while myosin II activity is required for the invasion of the MIA PaCa-2 and PANC-1 cells, other factors mediate the invasion of Hs766T cells.

#### *Hs766T Cells are Slower to Round Upon Detachment, Indicating Reduced Actomyosin Force Generation*

After observing that pharmacologic inhibition of myosin II activity does not affect the invasion of Hs766T cells, we next probed myosin II activity using an independent assay: we measure the rate of cell

rounding after cells are detached from their substrate with trypsin (Fig. 2). Cells with higher levels of myosin II activity tend to have a faster rounding time compared to cells with reduced myosin II activity.<sup>84</sup> We find that MIA PaCa-2 cells have the slowest cell rounding rate, as indicated by the highest rounding time constant of  $151 \pm 23$  s (Fig. 2b); this is consistent with Mia PaCa-2 cells having the slowest invasion rate, which is further decreased by inhibiting myosin II activity. By contrast, the Hs766T and PANC-1 cells round more quickly, as indicated by their shorter rounding time constants of  $118 \pm 12$  s and  $82 \pm 12$  s (Fig. 2b). With blebbistatin treatment, the cell rounding rate is reduced the most for the MIA PaCa-2 and PANC-1 cells. The MIA PaCa-2 cells show a 3-fold increase in rounding time constants, while the PANC-1 exhibit a larger 107-fold increase. These results are consistent with the marked decrease in invasion of these cell lines with myosin II inhibition (Fig. 1). Interestingly, the Hs766T cells show a much smaller  $\sim 2$ -fold increase in the rounding time constant with blebbistatin treatment (Fig. 2b), which corroborates our observations of blebbistatin effects on invasion and further substantiates that MIA PaCa-2 and PANC-1 cells are more dependent on myosin II activity to generate forces compared to Hs766T cells.

These data further underscore the differential effects of myosin II inhibition across different cell lines and suggest that force generation by Hs766T cells during invasion may occur through another mechanism.

#### *PANC-1 Cells Exert Increased Traction Stresses Compared to Hs766T Cells*

The ability of cells to generate traction forces on the surrounding extracellular matrix is critical during many modes of cancer cell invasion.<sup>48</sup> More invasive cells tend to exhibit increased traction stresses.<sup>47</sup> Thus, since Hs766T cells are the most invasive cell line, we initially predicted that these cells would have increased traction stresses compared to the other PDAC cell lines. However, traction force generation is influenced by myosin II activity, which does not appear to be a dominant mechanism of force generation in Hs766T cells based on our cell invasion and rounding experiments with blebbistatin treatment. To further explore the mechanisms of force generation in PDAC cells, we quantify traction stresses that cells exert on their substrate using a micropillar assay in which cells are plated on polydimethylsiloxane (PDMS) micropillars (Fig. 3a) that have a well-characterized elastic modulus.<sup>111</sup> In our micropillar assay, the average force per

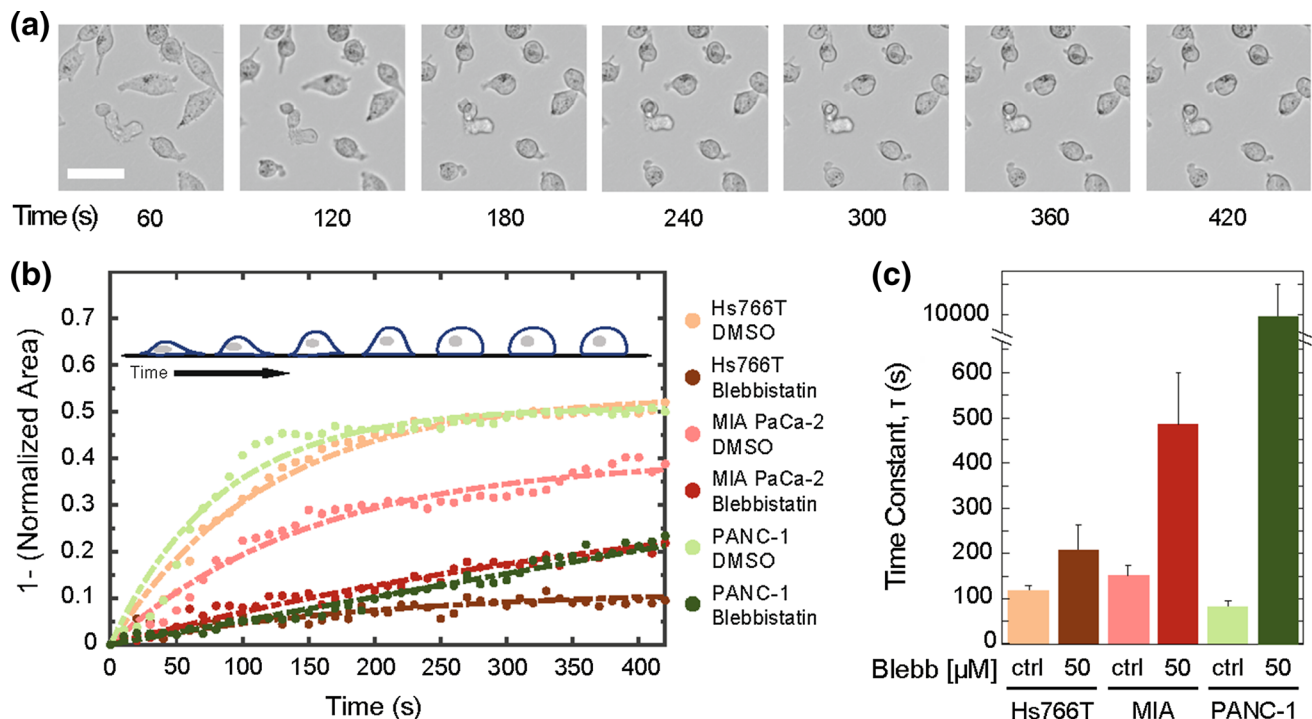


**FIGURE 2.** Myosin II activity contributions to cell rounding rate vary across cell lines. (a) Representative images show time sequence of MIA PaCa-2 cell shape change following the addition of trypsin. Scale,  $10 \mu\text{m}$ . (b) Quantification of cell area as a function of time for cells treated with DMSO (ctrl) and  $50 \mu\text{M}$  blebbistatin PDAC cells. Insert represents rounding cell over time. Dashed lines indicate fits with a bounded exponential growth model used to extract: (c) rounding time constants,  $\tau$ . Cells are treated with  $50 \mu\text{M}$  blebbistatin for 30 min prior to trypsinization. Data points show averages of at least 21 cells across three independent experiments. Error bars represent the 95% confidence intervals.

area (stress) exerted by cells is calculated by measuring the displacements of the micropillars. We find that the average traction stress exerted by PANC-1 cells is  $44 \pm 7 \text{ nN}/\mu\text{m}^2$  while Hs766T cells have a 38% lower average traction stress of  $27 \pm 7 \text{ nN}/\mu\text{m}^2$  ( $p = 1.0 \times 10^{-5}$ ) (Figs. 3b and 3c). These findings corroborate our observations that PANC-1 cells round more quickly than Hs766T cells, as both assays depend on actomyosin activity. We next determine contributions of myosin II to cellular traction forces by treating cells with blebbistatin. For the PANC-1 cells, we find that the average traction stress decreases by 30% following blebbistatin treatment ( $p = 2.8 \times 10^{-4}$ ) (Figs. 3b and 3c). Our results with the blebbistatin-treated PANC-1 cells are consistent with previous studies showing that myosin II activity is a major contributor to traction force generation.<sup>7,57</sup> By contrast, the Hs766T cells do not show a significant change in average traction stress with pharmacologic inhibition of myosin II ( $26 \pm 7 \text{ nN}/\mu\text{m}^2$  for the vehicle control cells vs.  $28 \pm 7 \text{ nN}/\mu\text{m}^2$  for the blebbistatin-treated cells,  $p = 3.7 \times 10^{-1}$ ) (Figs. 3b and 3c). Thus, our findings substantiate the differential contributions of myosin II activity to the forces generated by PANC-1 and Hs766T cells, and further suggest that Hs766T

cells may be using an invasion strategy that does not depend on myosin II.

### Myosin II Activity Contributes to PDAC Cell Stiffness

To further investigate the relationship between cell invasion and cell stiffness, we next determine the contributions of myosin II activity to cellular stiffness. We use atomic force microscopy (AFM) to measure the elastic modulus,  $E$ , of PDAC cells with and without the myosin II inhibitor blebbistatin. With the control DMSO treatment, Hs766T cells are nearly twofold stiffer than PANC-1 cells (Fig. 4a), which is consistent with our previous measurements of untreated cells.<sup>61</sup> With inhibition of myosin II activity, we observe a significant  $\sim$ threefold reductions in the stiffness ( $E$ ) of both Hs766T and PANC-1 cells: Hs766T cell stiffness decreases from a median of 3.5 to 1.1 kPa ( $p = 3.0 \times 10^{-6}$ ), while PANC-1 cell stiffness decreases from a median of 2.0 to 0.7 kPa ( $p = 1.0 \times 10^{-5}$ ) (Fig. 4a). Our results are consistent with other observations that inhibition of myosin II activity makes adherent cells more deformable.<sup>95</sup> While we find a significant decrease in Hs766T cell stiffness with blebbistatin treatment, there are no sig-

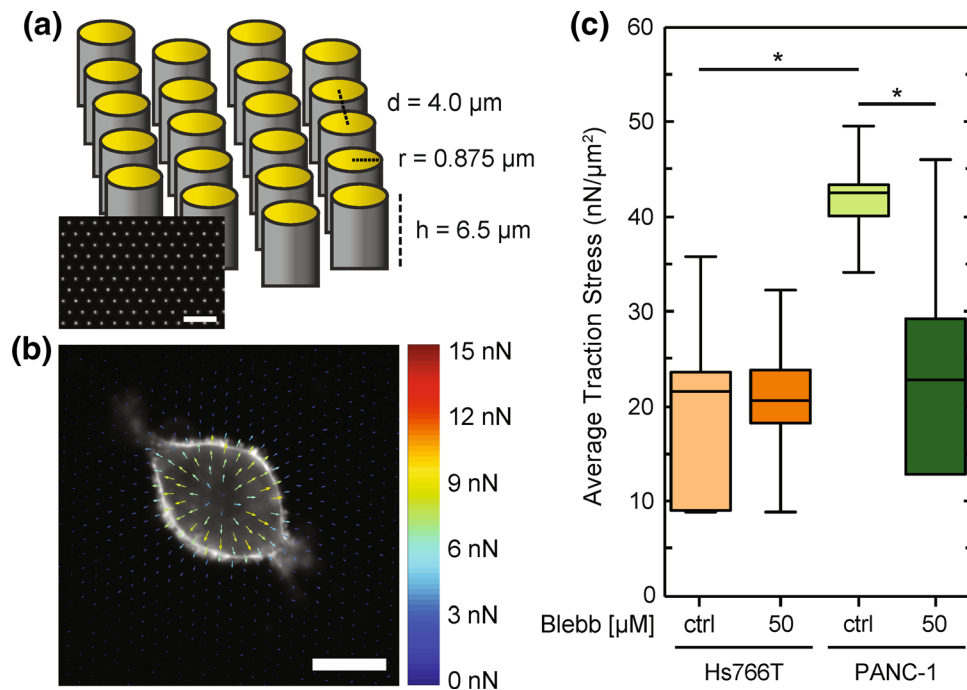


**FIGURE 3.** PANC-1 cells exert increased traction stresses compared to Hs766T cells. (a) Schematic illustration of the micropillar assay. Device dimensions are indicated for the distance between pillars  $d$ , as well as pillar radius  $r$  and height  $h$ . (b) Representative force map of a cell. Shown here is a PANC-1 cell treated with DMSO (ctrl) for 30 min prior to fixation. Average traction stress per cell is determined by analysis of the displacement of each gold-coated micropillar 18 h after plating of cells. (c) Box plots show the distribution of average traction stress per cell exerted by Hs766T and PANC-1 cells with and without blebbistatin treatment (50  $\mu\text{M}$ ). Boxes represent the 25th and 75th percentiles, whiskers represent the 10th and 90th percentiles, and the horizontal line represents the median.  $p$  values are determined by a Mann–Whitney U test.  $*p < 0.05$ . We measure traction stresses for at least 18 cells across three independent experiments.



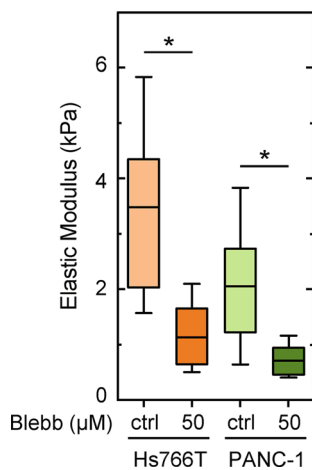


**FIGURE 4. Myosin II activity contributes to PDAC cell stiffness.** The elastic modulus,  $E$ , of PDAC cells adhered to Matrigel-coated glass is measured using atomic force microscopy (AFM) after cells are treated with DMSO (ctrl) or 50  $\mu\text{M}$  blebbistatin for 30 min. Each cell is measured with one indentation in the cytoplasmic region. Horizontal lines represent the average, boxes represent the 25th and 75th percentiles, and whiskers represent the 10th and 90th percentiles. Statistical significance is determined using a Mann–Whitney U test. \* $p < 0.05$ . Data represent 22–37 cells per treatment measured over three independent experiments.

nificant effects of myosin II inhibition on the invasion or traction force generation of these cells, suggesting that cell stiffness is not consistently associated with invasive potential.

#### *Invasion is not Altered by Matrix Metalloproteinase Inhibition*

We next investigate the activity of matrix metalloproteinases (MMPs) across PDAC cells as a possible explanation of why Hs766T cells are stiff and highly invasive but do not rely on myosin II for invasion. MMPs are major contributors to myosin II-independent modes of cancer cell invasion, as these enzymes degrade the surrounding protein matrix and thereby enlarge the size of gaps that cells must deform through during invasion.<sup>79,109</sup> The secretion of MMPs is also linked to the formation of invadopodia, which generate forces as they protrude from the plasma membrane.<sup>76</sup> If Hs766T cells have increased MMP production, this may explain why these cells are stiffer yet more invasive. To assess levels of MMPs across cell lines, we first analyze existing RNA-seq data.<sup>3</sup> We analyze levels of 23 MMP isoforms across Hs766T, MIA PaCa-2, and PANC-1 cell lines (Supp. Fig. 3A). Focusing on levels of the three MMPs that are most strongly implicated in the invasive potential of PDAC cells—*MMP2*, *MMP14*, *MMP28*<sup>1,73,86,120</sup>—we find that Hs766T cells have increased expression of *MMP14* compared to MIA PaCa-2 and PANC-1 cells

(145-fold and 36-fold higher), and an even higher expression of *MMP28* (1716-fold and 1274-fold higher). By contrast, *MMP2* expression is 4- and 425-fold higher in PANC-1 cells compared to Hs766T and MiaPaCa-2 cells.

While our gene expression analysis suggests that Hs766T cells have a higher overall level of MMP expression, levels of MMP expression do not always correlate to levels of MMP activity,<sup>66</sup> which is a functional measure of matrix degradation. Therefore, we next measure the activity of MMPs secreted from the PDAC cell lines using a fluorescence resonance energy transfer (FRET)-based MMP activity assay. We find that Hs766T cells have a 2.9-fold increase in MMP activity compared to MIA PaCa-2 cells ( $p = 7.5 \times 10^{-8}$ ) and a 1.5-fold increase compared to PANC-1 cells ( $p = 1.2 \times 10^{-5}$ ) (Supp. Fig. 3B). Thus, while Hs766T cells have only a slightly higher MMP activity level than PANC-1 cells, we hypothesized that this elevated MMP activity could contribute to their increased invasion and the insensitivity of their invasion to myosin II inhibition.

To directly test the role of MMP activity in PDAC cell invasion, we performed 3D invasion assays in the presence of the broad-spectrum MMP inhibitor GM6001. While treatment with 10 or 25  $\mu\text{M}$  GM6001 significantly decreases MMP activity across all three PDAC cell lines (Supp. Fig. 3B), we observe no significant effect of MMP inhibition on cell invasion (Supp. Fig. 3C). These results indicate that MMP activity does not contribute significantly to the invasion of these PDAC cell lines as measured by our Matrigel-based invasion assay. Our findings further illustrate that the increased invasion of Hs766T cells compared to other PDAC cell lines cannot be explained alone by their increased MMP activity and further support they are using an alternative force generation mechanism for invasion.

#### *Arp2/3 and Formin Activity Contribute to the Invasion of Hs766T Cells*

While increased myosin II activity can explain why PANC-1 cells are stiffer and more invasive than MIA PaCa-2 cells, it is still unclear what contributes to the concurrent increase in stiffness and invasion of Hs766T cells. We hypothesized that Hs766T cells may utilize alternative mechanisms for invasion that do not strongly rely on myosin II.<sup>60</sup> Another key mechanism of force generation is the formation of invadopodia, protrusive structures that contribute to cell invasion.<sup>29,31</sup> Two of the main components required for the formation of protrusions are Arp2/3 and formins, which mediate actin nucleation and branching. Thus, we hypothesized that the activity of Arp2/3 and for-

mins contributes to Hs766T cell invasion while myosin II-dependent forces are more critical for the invasion of MIA PaCa-2 and PANC-1 cells.

A characteristic hallmark of Arp2/3-dependent invasion is the formation of protrusions at the leading edge of an invading cell.<sup>94</sup> To determine if Hs766T cells exhibit any differences in protrusion formation compared to PANC-1 and MIA PaCa-2 cells, we quantify the length of the invasion front in our 3D scratch wound invasion assays (Supp. Fig. 4); a longer invasion front length indicates a greater number and/or length of protrusions, while a shorter front length reflects that the invading cell front exhibits fewer and/or shorter protrusions. Our analysis reveals that Hs766T cells have an average invasion front length of  $6283 \pm 1461 \mu\text{m}$  compared to  $3680 \pm 454 \mu\text{m}$  for MIA PaCa-2 cells ( $p = 9.2 \times 10^{-5}$ ) and  $3119 \pm 574 \mu\text{m}$  for PANC-1 cells ( $p = 4.1 \times 10^{-5}$ ) (Supp. Fig. 4). The increased length of the Hs766T invasion front supports the hypothesis that the invasion of these cells depends primarily on Arp2/3 activity, while MIA PaCa-2 and PANC-1 largely rely on myosin II activity to invade.

To determine the effects of Arp2/3 activity on PDAC cell invasion, we measure the invasion of cells treated with the Arp2/3 inhibitor, CK-666, which is a small molecule that stabilizes the inactive state of the Arp2/3 complex.<sup>35</sup> Comparing invasion across cell lines, we find that inhibition of Arp2/3 activity results in a slight but significant decrease in invasion for the MIA PaCa-2 and PANC-1 cells treated with  $50 \mu\text{M}$  CK-666 (MIA PaCa-2:  $11 \pm 2\%$  for DMSO-treated cells vs.  $9 \pm 2\%$  for  $50 \mu\text{M}$  CK-666,  $p = 3.9 \times 10^{-2}$ ; PANC-1:  $12 \pm 3\%$  for DMSO-treated cells vs.  $9 \pm 2\%$  for  $50 \mu\text{M}$  CK-666,  $p = 5.7 \times 10^{-3}$ ) (Figs. 5a and 5b). By contrast, we observe a greater, dose-dependent decrease in the invasion of Hs766T cells with increasing CK-666 concentration ( $23 \pm 7\%$  for DMSO-treated cells vs.  $19 \pm 5\%$  for  $20 \mu\text{M}$  CK-666 vs.  $15 \pm 5\%$  for  $50 \mu\text{M}$  CK-666; for DMSO vs.  $50 \mu\text{M}$  CK-666  $p = 2.1 \times 10^{-4}$ ) (Figs. 5a and 5b). We also measure effects of CK-666 on cell proliferation, which could impact the invasion assay findings, but observe there are no significant effects on proliferation over the invasion timescale of 24 h (Supp. Fig. 5A, 5B). Taken together, these results suggest that Arp2/3 activity contributes to the invasion of Hs766T cells but not significantly for PANC-1 or MIA PaCa-2 cells. By contrast, myosin II is a major contributor to the invasion of MIA PaCa-2 and PANC-1 cells, but has no significant effect on Hs766T cell invasion. These findings are consistent with the notion that different cell types rely on different mechanisms for invasion.<sup>67</sup>

While Arp2/3 is critical for actin nucleation and branching as well as cell motility, formins are also integral in actin nucleation and polymerization.<sup>71</sup> We

next investigate the role of formin activity in PDAC cell invasion by treating cells with SMIFH2, which broadly inhibits the family of formin proteins that are functionally important for cancer cell motility.<sup>41,78</sup> We find there is no significant difference in the invasion of MIA PaCa-2 and PANC-1 cells with SMIFH2 treatment compared to vehicle control (for  $50 \mu\text{M}$  at 24 h; MIA PaCa-2:  $p = 0.23$ , PANC-1:  $p = 0.91$ ) (Figs. 5c and 5d). We observe a small but significant difference in Hs766T cells treated with SMIFH2 compared to vehicle control ( $p = 2.6 \times 10^{-2}$ ). Moreover, we only find a difference in invasion of Hs766T cells with  $50 \mu\text{M}$  SMIFH2, unlike the dose-dependent effects of Arp2/3 inhibition. We further determine the effects of SMIFH2 on cell proliferation, which could impact the invasion assay results, and find there are no significant effects on proliferation over 24 h (Supp. Fig. 5C, 5D).

Taken together our results indicate that the activity of Arp2/3 is a major contributor to the invasion of Hs766T cells, while myosin II activity more heavily influences the invasion of MIA PaCa-2 and PANC-1 cells.

#### *Activity of Arp2/3 and Formins Contributes to Hs766T Cell Stiffness*

To determine the extent to which Arp2/3 and formin activity mediate cell stiffness, we next treat cells with either CK-666 or SMIFH2 and measure elastic modulus using AFM. Since Hs766T and PANC-1 cells are the most invasive and stiffest PDAC cell lines of our panel, we focus our measurements on these cell lines. Inhibiting Arp2/3 activity with CK-666 results in a significant decrease in the stiffness of Hs766T cells ( $p = 3.5 \times 10^{-3}$ ), but only a slight, insignificant decrease in PANC-1 stiffness ( $p = 5.5 \times 10^{-1}$ ) (Fig. 6a). Consistent with the effects of CK-666 treatment, inhibition of formin activity results in a greater reduction in stiffness of Hs766T than PANC-1 cells (Hs766T:  $p = 1.7 \times 10^{-2}$ , PANC-1:  $p = 2.2 \times 10^{-2}$ ) (Fig. 6c). Our AFM results confirm that the activity of both Arp2/3 and formins contribute to PDAC cell stiffness, indicating that actin nucleation, branching, and polymerization play a role in cell mechanotype.

To summarize our findings on the relationship between cell stiffness and invasion, we compile data for cell stiffness and invasion in a single plot (Fig. 7) and determine the strength of correlation across our panel of untreated PDAC cell lines and all drug perturbations at 24 h. We find that median values of invasion and cell stiffness across cell lines and treatment conditions are weakly correlated for Hs766T ( $R^2 = 0.34$ ) and for PANC-1 ( $R^2 = 0.30$ ) cells (Figs. 7a and 7b); compiling data for both cell types in a single plot yields a slightly higher but still weak correlation ( $R^2 = 0.45$ )

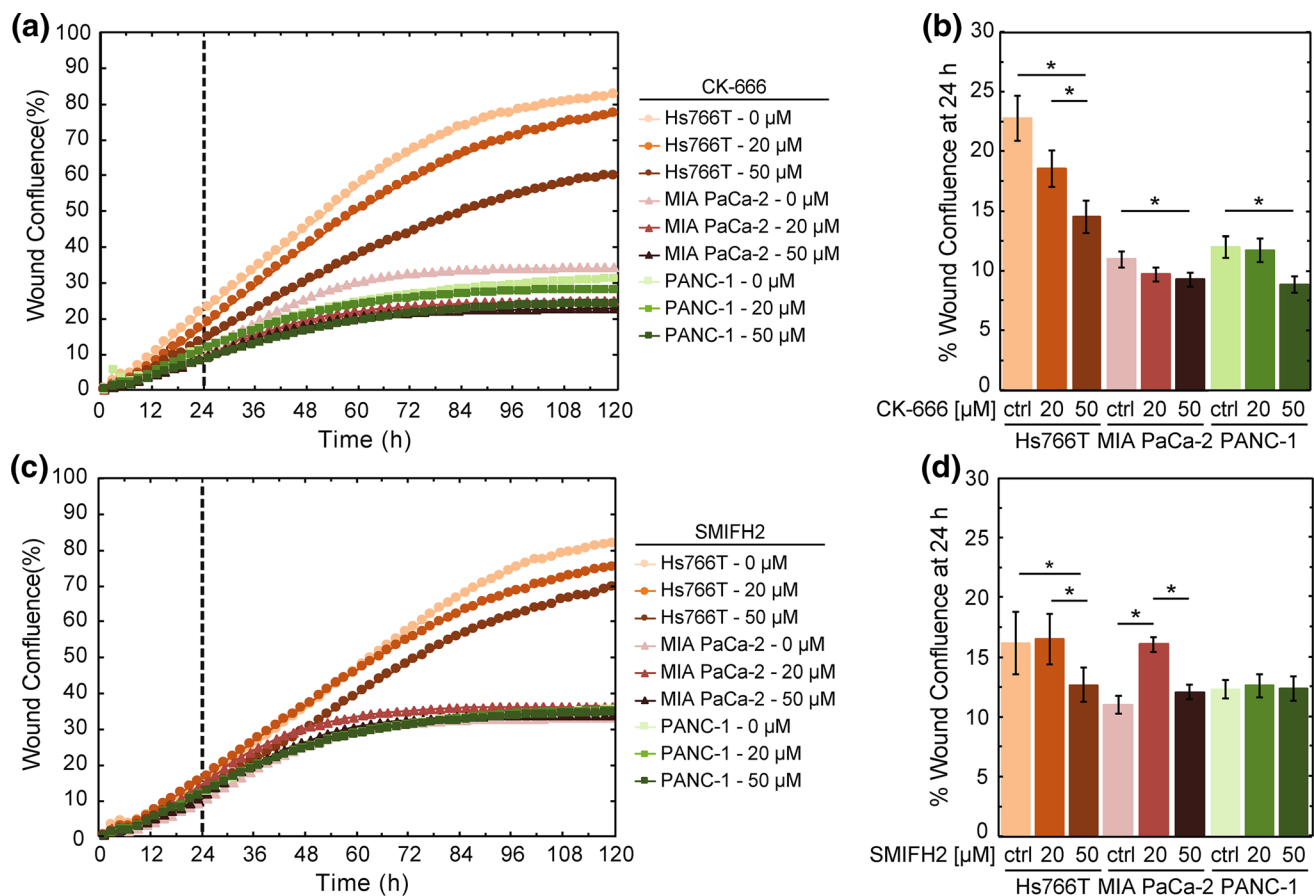


**FIGURE 5.** Activity of Arp2/3 contributes to the invasion of Hs766T cells. Invasion through Matrigel is measured by wound confluence in a 3D scratch wound invasion assay. Scatter plot shows the quantification of wound confluence over time with treatment of (a) the Arp2/3 inhibitor, CK-666 or (c) the formin inhibitor, SMIFH2. The dashed line indicates the 24 h time point, which we use to compare wound confluence values for statistical significance. Cells are treated with CK-666, SMIFH2, or DMSO (ctrl) from  $t = 0$ . Data points show average invasion over three independent experiments. Bar plot shows average wound confluence at the 24 h time point for (b) CK-666 or (d) SMIFH2 treated cells. Error bars represent standard error from three independent experiments. Pairwise  $p$  values are determined by a Student's  $t$  test. \* $p < 0.05$ .

(Fig. 7c). While this calculation neglects the sample variance, the lack of strong correlation demonstrates that these drug perturbations affect cell stiffness and invasion differently in different cell lines. Overall, these findings highlight how cell mechanotype and invasion are phenotypes that are influenced by multiple molecular mediators, and the factors that determine the phenotype in one cell type may not be the same for another cell type. For example, the activity of myosin II contributes to both contractile force generation<sup>24,65</sup> and actin crosslinking.<sup>49</sup> Therefore, the lack of strong correlation between stiffness and invasion could be explained by considering the multiple roles of myosin II: while myosin II inhibition does not affect Hs766T invasion or traction stresses, it may decrease Hs766T cell stiffness by reducing the crosslinking density of their actomyosin network.<sup>102</sup> By contrast, inhibition of myosin II activity in PANC-1 cells could reduce both crosslinking of actin and contractile force generation.

## DISCUSSION

Here we investigate the relationship between cell stiffness and invasion. We specifically study the role of myosin II, Arp2/3, and formin activity, as we hypothesized that these molecular components could contribute to the simultaneous increase in cell stiffness and invasion since they are involved in force generation. Our findings reveal that the activity of myosin II, Arp2/3, and formins contribute to the increased stiffness of PDAC cell lines; this may result from increased actomyosin contractility, actin polymerization and branching, and/or remodeling of the actin cytoskeleton. Indeed, the activity of Arp2/3<sup>5</sup> and myosin II<sup>44,45</sup> both contribute to the mechanical properties of reconstituted actin networks. Our observation that myosin II, Arp2/3, and formin activity contribute to cell stiffness are also consistent with previous *in vitro* studies of cancer cell lines.<sup>9,28,95</sup> For example, blebbistatin treatment of IGROV and Ovca429T $\beta$ R111

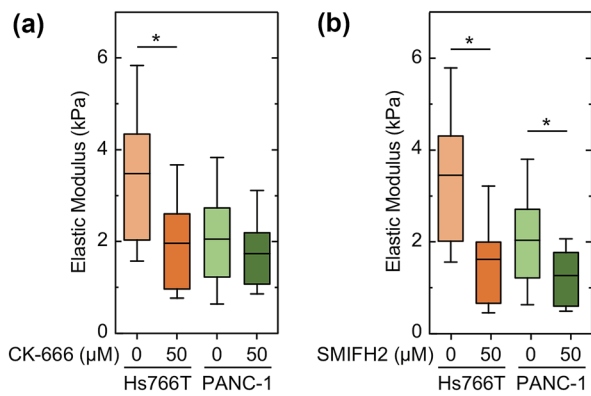


**FIGURE 6. Arp2/3 and formin activity contribute to PDAC cell stiffness.** The elastic modulus,  $E$ , of PDAC cells adhered to Matrigel-coated glass is measured using atomic force microscopy (AFM) when cells are treated with (a) 50  $\mu\text{M}$  CK-666 or (b) 50  $\mu\text{M}$  SMIFH2 for 30 minutes. Boxes represent the 25th and 75th percentiles, whiskers represent the 10th and 90th percentiles, and the horizontal line represents the median. Statistical significance calculated with Mann Whitney U test.  $*p < 0.05$ .

ovarian cancer cell lines reduce cell stiffness by  $\sim 50\%$ .<sup>95</sup> Since myosin II, Arp2/3, and formins are also essential crosslinkers and mediators of actin nucleation and branching, the decrease in cell stiffness that we observe when these components are inhibited could also result from a restructured actin cytoskeleton.

While inhibition of myosin II, Arp2/3, and formins have consistent effects on decreasing cell stiffness across Hs766T and PANC-1 cells, we discovered that inhibiting these proteins have varying effects on the invasion of different cell lines. We find that myosin II activity is a major contributor to PANC-1 cell invasion, while Hs766T cells are more dependent on the activity of Arp2/3 and formins. Our findings suggest that different pancreatic cancer cell lines utilize different strategies for invasion. It is plausible that these disparities stem from genetic differences, which may influence the response of cancer cells to pharmacologic inhibitors.<sup>6,98</sup> The three cancer cell lines that we investigate here—Hs766T, MIA PaCa-2, and PANC-1—are all pancreatic ductal epithelial cells that have undergone oncogenic transformation and have similar tissue origins but different genetic backgrounds. While all three cell lines carry common founder mutations in *KRAS*, *TP53*, and *CDKN2A*, the Hs766T cells have an additional *SMAD4* mutation, which is characteristic of higher grade lesions.<sup>17</sup> *SMAD4* encodes for a transcription factor that mediates signaling of the transforming growth factor (TGF)- $\beta$  superfamily of proteins.<sup>98</sup> Loss of Smad4 function in PDAC cells prevents TGF- $\beta$ -mediated suppression of EGFR promoter activity, triggering a signaling cascade that leads

to increased invasion.<sup>119</sup> Indeed, EGF-induced ERK activation regulates protrusion formation through the WAVE2 regulatory complex, which then activates Arp2/3.<sup>13</sup> It is intriguing to speculate that the Arp2/3-mediated invasion of Hs766T cells results from the loss of Smad4 activity. Indeed, the PANC-1 and MIA PaCa-2 cell lines have more similar genetic background and their invasion depends more strongly on myosin II activity. Our observations are aligned with previous findings that show cell line-specific differences in the influence of the Arp2/3 complex on the migration of pancreatic cancer cells.<sup>75</sup> Future studies investigating the relationship between genotype and phenotype across larger numbers of cell lines could enhance our ability to predict treatment response based on a cell's genotype. For example, our findings that Hs766T invasion is not affected by inhibition of myosin II could have consequences for treatments with inhibitors of Rho and ROCK, which have downstream effects on myosin II activity through a Rho-ROCK-NMII axis. Clinical trials with Fasudil show promise for patient benefit<sup>106</sup> and preclinical studies reveal that Rho inhibitors reduce cancer cell invasion *in vitro*.<sup>50,53</sup> Thus, our findings that inhibition of myosin II does not reduce invasion of *all* cancer cell types could have clinical relevance. A deeper knowledge of genome–phenome relationships, including which specific mutations are associated with specific mechanisms of force generation across cancer subtypes, could guide personalized treatments, in which drug combinations could be targeted to patients based on their genetic profile.

The differential effects of drug treatments on the invasion and stiffness across PDAC cell lines may also be explained by differences in the expression of genes and proteins that contribute to invasion and stiffness.<sup>11,117</sup> To determine if Hs766T cells have differential expression of genes encoding key proteins that are essential in cell invasion and stiffness, we analyzed existing RNA-seq data.<sup>3</sup> While Hs766T cells exhibited increased MMP expression and activity, we found no differences in invasion with MMP inhibition suggesting that Hs766T cells do not invade more quickly due to their increased MMP levels. Future work will provide more detailed insight into the relationship between MMP expression and the invasion of PDAC cells using knockdown and overexpression of specific MMP-encoding genes. The observed insensitivity of PDAC invasion to MMP inhibitors may also be due to the role of other proteases such as cathepsins, which are highly and specifically expressed in PDAC,<sup>33</sup> and could also contribute to the observed invasion. Since the forces that cells generate are critical for cells to invade and deform through a protein matrix, we also investigated expression levels of myosin IIA and IIB, which contribute to cell invasion. Hs766T cells had the

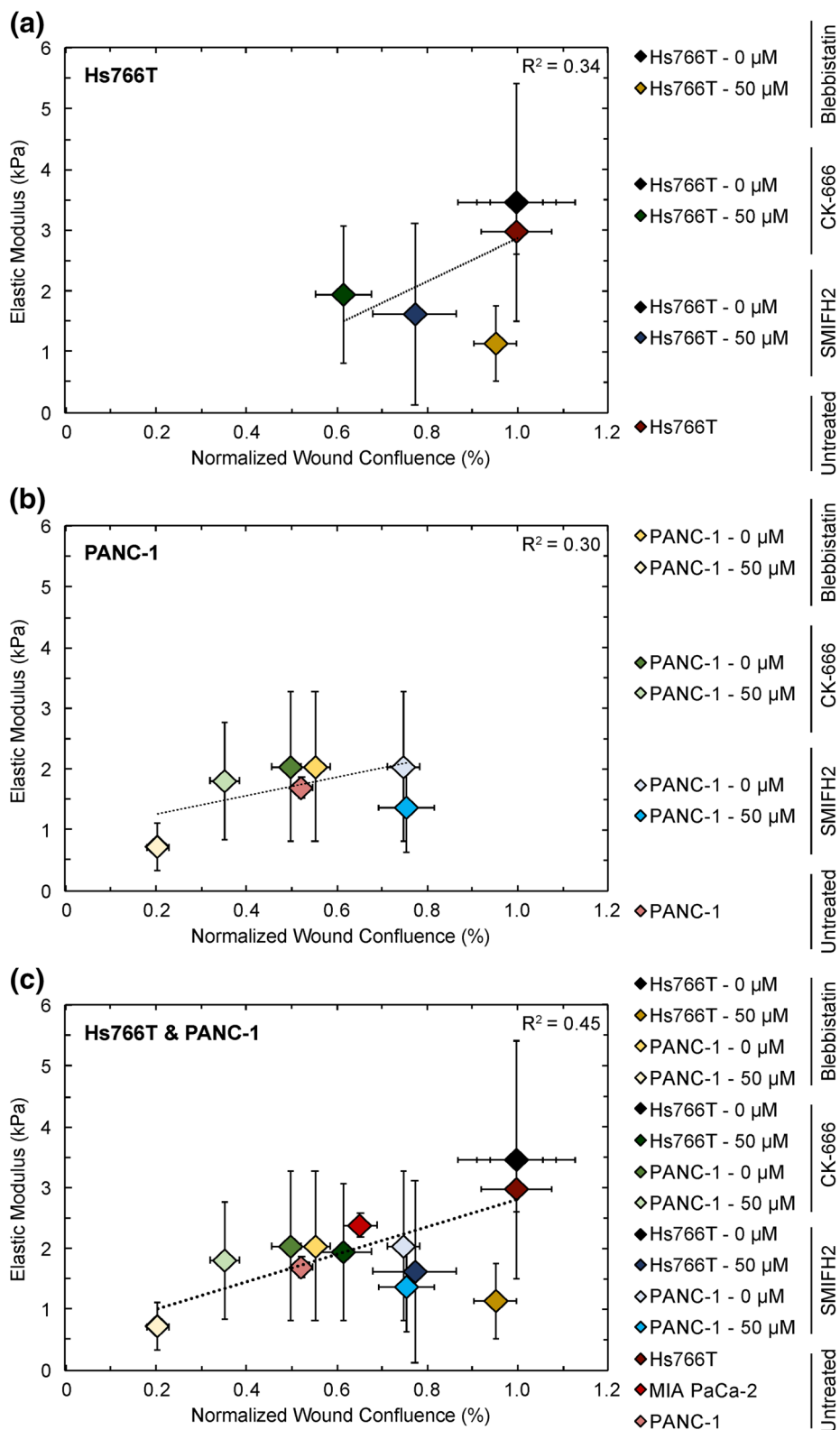


**FIGURE 7.** Linear regression of cellular elastic modulus vs. invasion, as measured as wound confluence by 3D scratch-wound invasion for untreated (a) Hs766T and (b) PANC-1 cells, as well as with treatments of blebbistatin, CK-666, or SMIFH2. (c) Compiled data for both Hs766T and PANC-1 cells. Median values and standard deviations are plotted here.  $R$  = Pearson's correlation coefficient determined by linear regression of median elastic modulus and wound confluence values across samples. Note that the sample variances were not included in calculating the correlation.

highest expression of MYH9 and MYH10, but the PANC-1 cells exhibit faster cell rounding and exert a greater magnitude of traction forces, which are both indicators of increased myosin-II dependent force generation. Our previous analysis of gene expression and protein levels of beta- and F-actin also did not reveal any distinct trends that explain the enhanced invasion of Hs766T cells.<sup>61</sup> These discrepancies between expression levels and cellular physical phenotypes highlight how such complex physical properties are challenging to fully explain by analysis of genetics or transcriptomics data alone. Deformability and contractility are emergent phenotypes that are determined by proteins, their higher-order structures, and dynamic remodeling processes. A deeper understanding of the molecules and pathways that regulate cell physical phenotypes, together with more sophisticated expression analysis, should make progress towards predicting physical phenotypes and ultimately cancer cell invasion and tumor progression.

### Measurement Effects

In addition to differences in the molecular machinery that influences stiffness and invasion, it is important to acknowledge how measurements of cell mechanotype and invasion may be affected by the experimental method. Measurements of cell stiffness can vary depending on the time and length scale of deformation, as well as the adhesion state of cells. In this study, we use AFM to measure the stiffness of cells that are adhered to a Matrigel-coated, glass surface, revealing that the stiffest to most compliant cells are Hs766T > PANC-1 > MIA PaCa-2. This relationship may differ if cell stiffness is measured using a different method. For example, we previously measured these same cells using the microfluidic-based method, quantitative deformability cytometry (q-DC),<sup>61,63</sup> and found that the ranking of cell stiffness from stiffest to most compliant was PANC-1 > Hs766T > MIA PaCa-2. There are differences in the time and length scales of deformations between AFM and q-DC—nanometer-scale deformations over seconds by AFM versus micron-scale deformations over milliseconds in q-DC—which could impact cell stiffness measurements.<sup>63</sup> Furthermore, cells are in a suspended state for q-DC and adhered for AFM, and there are clear differences in the intrinsic and extrinsic factors that determine cell mechanotype when cells are in an adhered versus suspended state. For example, when cells are adhered to their substrate *via* integrins and focal adhesions, the contractile forces they generate are transduced to the matrix, and bidirectional feedback with matrix stiffness can drive contractile force generation.<sup>58,90</sup> Increased myosin II activity subsequently

increases cell stiffness and invasion of cancer cells.<sup>69</sup> Indeed, cells with increased metastatic potential tend to exert higher levels of traction stresses.<sup>47</sup> The degree of cell spreading, which is influenced by Arp2/3 activity,<sup>34</sup> could also affect the stiffness of adhered cells. Fluidic methods, such as q-DC, measure cells in suspension, a state in which cortical actin<sup>82</sup> and the nucleus<sup>32,81</sup> are primary contributors to the deformation of cells through micron-scale pores. The mechanotype of suspended cells is also sensitive to myosin II activity,<sup>9,10</sup> suggesting that dynamic remodeling of the cytoskeleton may contribute to the stiffness of cells in a suspended state. Since metastasis requires cancer cells to both invade on solid substrates, such as through the extracellular matrix, and circulate in a suspended state, comparisons of the same cell types using multiple, complementary methods can provide a more integrated understanding of cancer cell physical properties and their impact on disease progression.

Cell invasion measurements may also depend on factors specific to the invasion assay. Here we measured invasion through a Matrigel matrix in a 3D scratch wound assay. Matrigel is rich in laminin and collagen IV, and therefore, has been widely used as a model to study invasion through basement membranes, such as those of the endothelium that cancer cells are required to penetrate in order to seed a metastatic site.<sup>38</sup> We cannot exclude that Matrigel might trigger a different invasion mode for Hs766T compared to PANC-1 cells. For example, both Rho/ROCK-dependent and -independent modes of invasion are determined by the spatial organization of surrounding collagen fibers.<sup>70</sup> Therefore, the invasion of these cells in a different matrix, such as collagen, which mimics interstitial stromal extracellular matrix,<sup>27</sup> could trigger cancer cells to use a different invasion strategy. Considering that PDAC progression also requires cells to invade through the confines of stromal interstitial matrices, future studies of the invasion of PDAC cells through collagen I, which is a major component of the tumor stroma, may capture other behaviors of PDAC cells. Indeed different invasion behaviors have been observed for ovarian cancer cells in a matrix of collagen I versus Matrigel.<sup>89</sup> The matrix composition can also impact the role of MMPs in invasion, as cell–matrix adhesions regulate MMP expression<sup>21,22,97</sup> and MMP activity may differentially contribute to cell invasion depending on the matrix material.<sup>89</sup> The role of MMPs in PDAC invasion also appears to depend on cell type: while we did not observe any effects of MMP inhibition on the invasion of PANC-1, MiaPaCa-2, or Hs766T cells, GM6001 treatment blocked the invasion of the related PDAC cell line, AsPC1.<sup>83,92</sup> Cells also adapt distinct invasion

modes that utilize different molecular machineries depending on whether the invasion is collective or individual.<sup>79</sup> Here we use a 3D scratch wound invasion assay, where cell invasion is measured by the collective movement of cells. While we have observed similar invasion results with 3D scratch wound and transwell migration assays,<sup>43</sup> previous reports cite differences in the invasion of cancer cells using transwell, scratch wound, 3D spheroid, and *in vivo* assays.<sup>62,89</sup> In the complex tumor microenvironment, fibroblasts, mast cells, and other cell types produce a number of molecules including cytokines, MMPs, and growth factors—such as vascular endothelial growth factor VEGF and basic fibroblast growth factor bFGF<sup>12,87,92</sup>—which additionally contribute to PDAC progression.<sup>38</sup> Future studies of PDAC invasion across different matrix materials and conditions will provide a more detailed understanding of the context-dependence of PDAC invasion, which could ultimately inform therapeutic interventions.

#### *Context-Dependent Relationship Between Cell Stiffness and Invasion*

Cellular mechanotype is emerging as a potential complementary biomarker for cancer diagnosis and prognosis. While many studies reveal that more invasive cells tend to be more compliant,<sup>15,25,56,112</sup> the positive correlation that we observe between PDAC cell stiffness and invasion is aligned with complementary findings in other cell types, including in lung cancer cells with varying metastatic potential,<sup>116</sup> as well as in breast cancer cells treated with agonists to activate beta-adrenergic signaling.<sup>43,61,74,116</sup> We previously found a strong correlation between the stiffness and invasion of PANC1, Hs766T, and MIA PaCa-2 cells.<sup>61</sup> In this study, we find only a weak correlation between the stiffness and invasion of PDAC cells treated with inhibitors of myosin II (blebbistatin), Arp2/3 (CK-666), or formins (SMIFH2); this suggests that the relationship between stiffness and invasion of cells induced by pharmacologic perturbations may be difficult to predict. A combination of physical phenotypes, such as deformability, contractility, and adhesion, rather than single parameters, could further enhance the use of physical phenotypes as indicators of invasion or metastatic potential. For example, multivariate analysis of physical phenotypes may enhance the ability to predict functional behaviors, such as invasion.<sup>64</sup>

## CONCLUSION

Our analysis of the relationship between cell mechanotype and invasion across PDAC cells with pharmacologic perturbations of actin and myosin provides deeper insights into mechanisms of cancer cell invasion. The cell-type specific effects of drugs on invasion that we observe reinforces the notion that different cells—even those derived from similar tissue origin—use different strategies for invasion. Given the genetic heterogeneity of cells within a single tumor and across different patients, as well as the phenotypic variability of isogenic cells, a better understanding of clinically relevant phenotypes such as invasion, as well as genotype–phenotype relationships should strengthen clinical strategies to develop therapies that target distinct mechanisms of cell invasion and metastasis.

## ACKNOWLEDGMENTS

We thank our funding sources: the National Science Foundation (CAREER DBI-1254185 and BMMB-1906165 to ACR), the Farber Family Foundation, and UCLA Integrative Biology & Physiology Eureka Scholarship (to AVN), and the National Institutes of Health (R01 GM110482 to MJB). We would also like to thank Timothy Donahue and his laboratory for their insights into PDAC, as well as their generous contributions of the PDAC cell lines used in our studies. We are also grateful to Gordon Robertson and Ewan Gibb for their bioinformatics expertise. The MMP activity assay was performed in the UCLA Molecular Shared Screening Resource in the California NanoSystems Institute with technical support from Robert Damoiseaux and Bobby Tofig.

## CONFLICT OF INTEREST

Angelyn V. Nguyen, Brittany Trompetto, Xing Haw Marvin Tan, Michael B. Scott, Kenneth Hsueh-heng Hu, Eric Deeds, Manish J. Butte, Pei Yu Chiou, and Amy C. Rowat have no conflicts of interest.

## ETHICAL STANDARDS

No human or animals studies were carried out by the authors for this article.

## REFERENCES

- <sup>1</sup>Ali, M. H., D. P. Pearlstein, C. E. Mathieu, P. T. Schumacker, H. Mir, and T. Paul. Mitochondrial requirement for endothelial responses to cyclic strain: implications for mechanotransduction. *Am. J. Physiol. Lung Cell. Mol. Physiol.* 60637:486–496, 2004.
- <sup>2</sup>Arjonen, A., *et al.* Mutant p53-associated myosin-X upregulation promotes breast cancer invasion and metastasis. *J. Clin. Invest.* 124:1069–1082, 2014.
- <sup>3</sup>Barretina, J., *et al.* The Cancer Cell Line Encyclopedia enables predictive modelling of anticancer drug sensitivity. *Nature* 483:603–607, 2012.
- <sup>4</sup>Beadle, C., M. C. Assanah, P. Monzo, R. Vallee, S. S. Rosenfeld, and P. Canoll. The role of myosin II in glioma invasion of the brain. *Mol. Biol. Cell* 19:3357–3368, 2008.
- <sup>5</sup>Bieling, P., *et al.* Force feedback controls motor activity and mechanical properties of self-assembling branched actin networks. *Cell* 164:115–127, 2016.
- <sup>6</sup>Bronte, G., *et al.* Driver mutations and differential sensitivity to targeted therapies: a new approach to the treatment of lung adenocarcinoma. *Cancer Treat. Rev.* 36(Suppl 3):S21–S29, 2010.
- <sup>7</sup>Burridge, K., and C. Guilluy. Focal adhesions, stress fibers and mechanical tension. *Exp. Cell Res.* 343:14–20, 2016.
- <sup>8</sup>Calzado-Martín, A., M. Encinar, J. Tamayo, M. Calleja, and A. San Paulo. Effect of actin organization on the stiffness of living breast cancer cells revealed by peak-force modulation atomic force microscopy. *ACS Nano* 10:3365–3374, 2016.
- <sup>9</sup>Cartagena-Rivera, A. X., J. S. Logue, C. M. Waterman, and R. S. Chadwick. Actomyosin cortical mechanical properties in nonadherent cells determined by atomic force microscopy. *Biophys. J.* 110:2528–2539, 2016.
- <sup>10</sup>Chan, C. J., *et al.* Myosin II activity softens cells in suspension. *Biophys. J.* 108:1856–1869, 2015.
- <sup>11</sup>Chan, C. K., *et al.* Tumour-suppressor microRNAs regulate ovarian cancer cell physical properties and invasive behaviour. *Open Biol.* 6:160275, 2016.
- <sup>12</sup>Chang, D. Z. Mast cells in pancreatic ductal adenocarcinoma. *OncImmunology* 1:754–755, 2012.
- <sup>13</sup>Chen, Y.-W., *et al.* SMAD4 Loss triggers the phenotypic changes of pancreatic ductal adenocarcinoma cells. *BMC Cancer* 14:181, 2014.
- <sup>14</sup>Chin, L., Y. Xia, D. E. Discher, and P. A. Janmey. Mechanotransduction in cancer. *Curr. Opin. Chem. Eng.* 11:77–84, 2016.
- <sup>15</sup>Cross, S. E., Y.-S. Jin, J. Rao, and J. K. Gimzewski. Nanomechanical analysis of cells from cancer patients. *Nat. Nanotechnol.* 2:780–783, 2007.
- <sup>16</sup>Cuadrado, A., Z. Martin-Moldes, J. Ye, and I. Lastres-Becker. Transcription factors NRF2 and NF- $\kappa$ B are coordinated effectors of the rho family, GTP-binding protein RAC1 during inflammation. *J. Biol. Chem.* 289:15244–15258, 2014.
- <sup>17</sup>Deer, E. L., *et al.* Phenotype and genotype of pancreatic cancer cell lines. *Pancreas* 39:425–435, 2010.
- <sup>18</sup>Denaïs, C. M., *et al.* Nuclear envelope rupture and repair during cancer cell migration. *Science* 352:353–358, 2016.
- <sup>19</sup>Dobin, A., *et al.* STAR: ultrafast universal RNA-seq aligner. *Bioinformatics* 29:15–21, 2013.
- <sup>20</sup>Duxbury, M. S., S. W. Ashley, and E. E. Whang. Inhibition of pancreatic adenocarcinoma cellular invasiveness by blebbistatin: a novel myosin II inhibitor. *Biochem. Biophys. Res. Commun.* 313:992–997, 2004.
- <sup>21</sup>Ellerbroek, S. M., Y. I. Wu, C. M. Overall, and M. S. Stack. Functional interplay between type I collagen and cell surface matrix metalloproteinase activity. *J. Biol. Chem.* 276:24833–24842, 2001.
- <sup>22</sup>Ellerbroek, S. M., *et al.* Ovarian carcinoma regulation of matrix metalloproteinase-2 and membrane type 1 matrix metalloproteinase through beta1 integrin. *Cancer Res.* 59:1635–1641, 1999.
- <sup>23</sup>Engler, A. J., S. Sen, H. L. Sweeney, and D. E. Discher. Matrix elasticity directs stem cell lineage specification. *Cell* 126:677–689, 2006.
- <sup>24</sup>Even-Ram, S., A. D. Doyle, M. A. Conti, K. Matsumoto, R. S. Adelstein, and K. M. Yamada. Myosin IIA regulates cell motility and actomyosin-microtubule crosstalk. *Nat. Cell Biol.* 9:299–309, 2007.
- <sup>25</sup>Faria, E. C., *et al.* Measurement of elastic properties of prostate cancer cells using AFM. *Analyst* 133:1498, 2008.
- <sup>26</sup>Fletcher, D. A., and R. D. Mullins. Cell mechanics and the cytoskeleton. *Nature* 463:485–492, 2010.
- <sup>27</sup>Frantz, C., K. M. Stewart, and V. M. Weaver. The extracellular matrix at a glance. *J. Cell Sci.* 123:4195–4200, 2010.
- <sup>28</sup>Fritzsche, M., C. Erlenkämper, E. Moeendarbary, G. Charras, and K. Kruse. Actin kinetics shapes cortical network structure and mechanics. *Sci. Adv.* 2:e1501337, 2016.
- <sup>29</sup>Gardberg, M., *et al.* FHOD1, a formin upregulated in epithelial-mesenchymal transition, participates in cancer cell migration and invasion. *PLoS ONE* 8:e74923, 2013.
- <sup>30</sup>Gardel, M. L., I. C. Schneider, Y. Aratyn-Schaus, and C. M. Waterman. Mechanical integration of actin and adhesion dynamics in cell migration. *Annu. Rev. Cell Dev. Biol.* 26:315–333, 2010.
- <sup>31</sup>Goley, E. D., and M. D. Welch. The ARP2/3 complex: an actin nucleator comes of age. *Nat. Rev. Mol. Cell Biol.* 7:713–726, 2006.
- <sup>32</sup>Harada, T., *et al.* Nuclear lamin stiffness is a barrier to 3D migration, but softness can limit survival. *J. Cell Biol.* 204:669–682, 2014.
- <sup>33</sup>Harsha, H. C., *et al.* A compendium of potential biomarkers of pancreatic cancer. *PLoS Med.* 6:e1000046, 2009.
- <sup>34</sup>Henson, J. H., *et al.* Arp2/3 complex inhibition radically alters lamellipodial actin architecture, suspended cell shape, and the cell spreading process. *Mol. Biol. Cell* 26:887–900, 2015.
- <sup>35</sup>Hetrick, B., M. S. Han, L. A. Helgeson, and B. J. Nolen. Small molecules CK-666 and CK-869 inhibit actin-related protein 2/3 complex by blocking an activating conformational change. *Chem. Biol.* 20:701–712, 2013.
- <sup>36</sup>Jaqaman, K., and S. Grinstein. Regulation from within: the cytoskeleton in transmembrane signaling. *Trends Cell Biol.* 22:515–526, 2012.
- <sup>37</sup>Jimenez Valencia, A. M., *et al.* Collective cancer cell invasion induced by coordinated contractile stresses. *Oncotarget* 6:43438–43451, 2015.
- <sup>38</sup>Kalluri, R. Basement membranes: structure, assembly and role in tumour angiogenesis. *Nat. Rev. Cancer* 3:422–433, 2003.
- <sup>39</sup>Katt, M. E., A. L. Placone, A. D. Wong, Z. S. Xu, and P. C. Searson. In vitro tumor models: advantages, disadvantages, variables, and selecting the right platform. *Front. Bioeng. Biotechnol.* 4:12, 2016.



- <sup>40</sup>Kim, S., and P. A. Coulombe. Emerging role for the cytoskeleton as an organizer and regulator of translation. *Nat. Rev. Mol. Cell Biol.* 11:75–81, 2010.
- <sup>41</sup>Kim, H.-C., Y.-J. Jo, N.-H. Kim, and S. Namgoong. Small molecule inhibitor of formin homology 2 domains (SMIFH2) reveals the roles of the formin family of proteins in spindle assembly and asymmetric division in mouse oocytes. *PLoS ONE* 10:e0123438, 2015.
- <sup>42</sup>Kim, T.-H., A. C. Rowat, and E. K. Sloan. Neural regulation of cancer: from mechanobiology to inflammation. *Clin. Transl. Immunol.* 5:e78, 2016.
- <sup>43</sup>Kim, T.-H., *et al.* Cancer cells become less deformable and more invasive with activation of  $\beta$ -adrenergic signaling. *J. Cell Sci.* 129:4563–4575, 2016.
- <sup>44</sup>Koenderink, G. H., *et al.* An active biopolymer network controlled by molecular motors. *Proc. Natl. Acad. Sci. USA* 106:15192–15197, 2009.
- <sup>45</sup>Köhler, S., A. R. Bausch, M. Welch, J. Peloquin, and T. Svitkina. Contraction mechanisms in composite active actin networks. *PLoS ONE* 7:e39869, 2012.
- <sup>46</sup>Kovács, M., J. Tóth, C. Hetényi, A. Málnási-Csizmadia, and J. R. Sellers. Mechanism of blebbistatin inhibition of myosin II. *J. Biol. Chem.* 279:35557–35563, 2004.
- <sup>47</sup>Kraning-Rush, C. M., J. P. Califano, and C. A. Reinhart-King. Cellular traction stresses increase with increasing metastatic potential. *PLoS ONE* 7:e32572, 2012.
- <sup>48</sup>Kumar, S., and V. M. Weaver. Mechanics, malignancy, and metastasis: the force journey of a tumor cell. *Cancer Metastasis Rev.* 28:113–127, 2009.
- <sup>49</sup>Laevsky, G., and D. A. Knecht. Cross-linking of actin filaments by myosin II is a major contributor to cortical integrity and cell motility in restrictive environments. *J. Cell Sci.* 116:3761–3770, 2003.
- <sup>50</sup>Liu, S., R. H. Goldstein, E. M. Scepansky, and M. Rosenblatt. Inhibition of rho-associated kinase signaling prevents breast cancer metastasis to human bone. *Cancer Res.* 69:8742–8751, 2009.
- <sup>51</sup>Lopez, J. I., I. Kang, W.-K. You, D. M. McDonald, and V. M. Weaver. In situ force mapping of mammary gland transformation. *Integr. Biol.* 3:910, 2011.
- <sup>52</sup>Maly, I. V., T. M. Domaradzki, V. A. Gossy, and W. A. Hofmann. Myosin isoform expressed in metastatic prostate cancer stimulates cell invasion. *Sci. Rep.* 7:8476, 2017.
- <sup>53</sup>Matsubara, M., and M. J. Bissell. Inhibitors of Rho kinase (ROCK) signaling revert the malignant phenotype of breast cancer cells in 3D context. *Oncotarget.* 7:31602–31622, 2016.
- <sup>54</sup>McBeath, R., D. M. Pirone, C. M. Nelson, K. Bhadriraju, and C. S. Chen. Cell shape, cytoskeletal tension, and RhoA regulate stem cell lineage commitment. *Dev. Cell* 6:483–495, 2004.
- <sup>55</sup>Mendez, M. G., S.-I. Kojima, and R. D. Goldman. Vimentin induces changes in cell shape, motility, and adhesion during the epithelial to mesenchymal transition. *FASEB J.* 24:1838–1851, 2010.
- <sup>56</sup>Mey, I., A. Janshoff, J. Rother, and H. No. Atomic force microscopy-based microrheology reveals significant differences in the viscoelastic response between malign and benign cell lines. *Open Biol.* 4:140046, 2014.
- <sup>57</sup>Mierke, C., D. Rosel, B. Fabry, and J. Brabek. Contractile forces in tumor cell migration. *Eur. J. Cell Biol.* 87:669–676, 2008.
- <sup>58</sup>Mih, J. D., A. Marinkovic, F. Liu, A. S. Sharif, and D. J. Tschumperlin. Matrix stiffness reverses the effect of actomyosin tension on cell proliferation. *J. Cell Sci.* 125:5974–5983, 2012.
- <sup>59</sup>Murrell, M., P. W. Oakes, M. Lenz, and M. L. Gardel. Forcing cells into shape: the mechanics of actomyosin contractility. *Nat. Rev. Mol. Cell Biol.* 16:486–498, 2015.
- <sup>60</sup>Nakayama, M., *et al.* Rho-kinase and myosin II activities are required for cell type and environment specific migration. *Genes Cells* 10:107–117, 2005.
- <sup>61</sup>Nguyen, A. V., *et al.* Stiffness of pancreatic cancer cells is associated with increased invasive potential. *Integr. Biol.* 8:1232–1245, 2016.
- <sup>62</sup>Noël, A. C., *et al.* Invasion of reconstituted basement membrane matrix is not correlated to the malignant metastatic cell phenotype. *Cancer Res.* 51:405–414, 1991.
- <sup>63</sup>Nyberg, K. D., K. H. Hu, S. H. Kleinman, D. B. Khismatullin, M. J. Butte, and A. C. Rowat. Quantitative deformability cytometry (q-DC): rapid measurements of single cell viscoelastic properties. *Biophys. J.* 113:1574–1584, 2017.
- <sup>64</sup>Nyberg, K. D., *et al.* Predicting cancer cell invasion by single-cell physical phenotyping. *Integr. Biol.* 10:218–231, 2018.
- <sup>65</sup>Ouderkirk, J. L., and M. Krendel. Non-muscle myosins in tumor progression, cancer cell invasion, and metastasis. *Cytoskeleton* 71:447–463, 2014.
- <sup>66</sup>Page-McCaw, A., A. J. Ewald, and Z. Werb. Matrix metalloproteinases and the regulation of tissue remodeling. *Nat. Rev. Mol. Cell Biol.* 8:221–233, 2007.
- <sup>67</sup>Krakhmal, N. V., M. V. Zavyalova, E. V. Denisov, S. V. Vtorushin, and V. M. Perelmuter. Cancer invasion: patterns and mechanisms. *Acta Nat.* 7:17–28, 2015.
- <sup>68</sup>Plodinec, M., *et al.* The nanomechanical signature of breast cancer. *Nat. Nanotechnol.* 7:757–765, 2012.
- <sup>69</sup>Poincloux, R., *et al.* Contractility of the cell rear drives invasion of breast tumor cells in 3D Matrigel. *Proc. Natl. Acad. Sci. USA* 108:1943–1948, 2011.
- <sup>70</sup>Provenzano, P. P., D. R. Inman, K. W. Eliceiri, S. M. Trier, and P. J. Keely. Contact guidance mediated three-dimensional cell migration is regulated by Rho/ROCK-dependent matrix reorganization. *Biophys. J.* 95:5374–5384, 2008.
- <sup>71</sup>Pruyne, D., *et al.* Role of formins in actin assembly: nucleation and barbed-end association. *Science* 297:612–615, 2002.
- <sup>72</sup>Raab, M., *et al.* ESCRT III repairs nuclear envelope ruptures during cell migration to limit DNA damage and cell death. *Science* 352:359–362, 2016.
- <sup>73</sup>Rasheed, Z. A., W. Matsui, and A. Maitra. Pathology of pancreatic stroma in PDAC. In: *Pancreatic Cancer and Tumor Microenvironment*, edited by P. J. Grippo, and H. G. Munshi. Trivandrum: Transworld Research Network, 2012.
- <sup>74</sup>Rathje, L.-S. Z., *et al.* Oncogenes induce a vimentin filament collapse mediated by HDAC6 that is linked to cell stiffness. *Proc. Natl. Acad. Sci. USA* 111:1515–1520, 2014.
- <sup>75</sup>Rauhala, H. E., S. Teppo, S. Niemelä, and A. Kallioniemi. Silencing of the ARP2/3 complex disturbs pancreatic cancer cell migration. *Anticancer Res.* 33:45–52, 2013.
- <sup>76</sup>Revach, O.-Y., A. Weiner, K. Rechav, I. Sabanay, A. Livne, and B. Geiger. Mechanical interplay between invadopodia and the nucleus in cultured cancer cells. *Sci. Rep.* 5:9466, 2015.
- <sup>77</sup>Ridley, A. J. RhoA, RhoB and RhoC have different roles in cancer cell migration. *J. Microsc.* 251:242–249, 2013.

- <sup>78</sup>Rizvi, S. A., *et al.* Identification and characterization of a small molecule inhibitor of formin-mediated actin assembly. *Chem. Biol.* 16:1158–1168, 2009.
- <sup>79</sup>Rodriguez-Hernandez, I., G. Cantelli, F. Bruce, and V. Sanz-Moreno. Rho, ROCK and actomyosin contractility in metastasis as drug targets. *Fl1000Research* 5:783, 2016.
- <sup>80</sup>Rowat, A. C., J. Lammerding, H. Herrmann, and U. Aebi. Towards an integrated understanding of the structure and mechanics of the cell nucleus. *BioEssays* 30:226–236, 2008.
- <sup>81</sup>Rowat, A. C., *et al.* Nuclear envelope composition determines the ability of neutrophil-type cells to passage through micron-scale constrictions. *J. Biol. Chem.* 288:8610–8618, 2013.
- <sup>82</sup>Salbreux, G., G. Charras, and E. Paluch. Actin cortex mechanics and cellular morphogenesis. *Trends Cell Biol.* 22:536–545, 2012.
- <sup>83</sup>Sato, N., N. Maehara, G. H. Su, and M. Goggins. Effects of 5-Aza-2'-deoxycytidine on matrix metalloproteinase expression and pancreatic cancer cell invasiveness. *J. Natl. Cancer Inst.* 95:327–330, 2003.
- <sup>84</sup>Sen, S., and S. Kumar. Cell-matrix de-adhesion dynamics reflect contractile mechanics. *Cell. Mol. Bioeng.* 2:218–230, 2009.
- <sup>85</sup>Shi, Q., *et al.* A novel low-molecular weight inhibitor of focal adhesion kinase, TAE226, inhibits glioma growth. *Mol. Carcinog.* 46:488–496, 2007.
- <sup>86</sup>Shields, M. A., S. Dangi-Garimella, S. B. Krantz, D. J. Bentrem, and H. G. Munshi. Pancreatic cancer cells respond to type I collagen by inducing snail expression to promote membrane type 1 matrix metalloproteinase-dependent collagen invasion. *J. Biol. Chem.* 286:10495–10504, 2011.
- <sup>87</sup>Sipos, B., *et al.* Vascular endothelial growth factor mediated angiogenic potential of pancreatic ductal carcinomas enhanced by hypoxia: an *in vitro* and *in vivo* study. *Int. J. Cancer* 102:592–600, 2002.
- <sup>88</sup>Smith, B. A., B. Tolloczko, J. G. Martin, and P. Grütter. Probing the viscoelastic behavior of cultured airway smooth muscle cells with atomic force microscopy: stiffening induced by contractile agonist. *Biophys. J.* 88:2994–3007, 2005.
- <sup>89</sup>Sodek, K. L., T. J. Brown, and M. J. Ringuette. Collagen I but not Matrigel matrices provide an MMP-dependent barrier to ovarian cancer cell penetration. *BMC Cancer* 8:223, 2008.
- <sup>90</sup>Southern, B. D., *et al.* Matrix-driven myosin II mediates the pro-fibrotic fibroblast phenotype. *J. Biol. Chem.* 291:6083–6095, 2016.
- <sup>91</sup>Stossel, T. P., and J. H. Hartwig. Filling gaps in signaling to actin cytoskeletal remodeling. *Dev. Cell* 4:444–445, 2003.
- <sup>92</sup>Strouch, M. J., *et al.* Crosstalk between mast cells and pancreatic cancer cells contributes to pancreatic tumor progression. *Clin. Cancer Res.* 16:2257–2265, 2010.
- <sup>93</sup>Suraneni, P., B. Rubinstein, J. R. Unruh, M. Durnin, D. Hanein, and R. Li. The Arp2/3 complex is required for lamellipodia extension and directional fibroblast cell migration. *J. Cell Biol.* 197:239–251, 2012.
- <sup>94</sup>Suraneni, P., *et al.* A mechanism of leading-edge protrusion in the absence of Arp2/3 complex. *Mol. Biol. Cell* 26:901–912, 2015.
- <sup>95</sup>Swaminathan, V., K. Mythreye, E. Tim O'Brien, A. Berchuck, G. C. Blobe, and R. Superfine. Mechanical stiffness grades metastatic potential in patient tumor cells and in cancer cell lines. *Cancer Res.* 71:5075–5080, 2011.
- <sup>96</sup>Swift, J., *et al.* Nuclear lamin-A scales with tissue stiffness and enhances matrix-directed differentiation. *Science* 341:1240104, 2013.
- <sup>97</sup>Symowicz, J., *et al.* Engagement of collagen-binding integrins promotes matrix metalloproteinase-9-dependent E-cadherin ectodomain shedding in ovarian carcinoma cells. *Cancer Res.* 67:2030–2039, 2007.
- <sup>98</sup>Takai, E., and S. Yachida. Genomic alterations in pancreatic cancer and their relevance to therapy. *World J. Gastrointest. Oncol.* 7:250–258, 2015.
- <sup>99</sup>Tan, J. L., J. Tien, D. M. Pirone, D. S. Gray, K. Bhadriraju, and C. S. Chen. Cells lying on a bed of microneedles: An approach to isolate mechanical force. *Proc. Natl. Acad. Sci. USA* 100:1484–1489, 2003.
- <sup>100</sup>Trapnell, C., *et al.* Transcript assembly and quantification by RNA-Seq reveals unannotated transcripts and isoform switching during cell differentiation. *Nat. Biotechnol.* 28:511–515, 2010.
- <sup>101</sup>Tse, H. T. K., *et al.* Quantitative diagnosis of malignant pleural effusions by single-cell mechanophenotyping. *Sci. Transl. Med.* 5:212ra163, 2013.
- <sup>102</sup>Tseng, Y., *et al.* How actin crosslinking and bundling proteins cooperate to generate an enhanced cell mechanical response. *Biochem. Biophys. Res. Commun.* 334:183–192, 2005.
- <sup>103</sup>Unbekandt, M., *et al.* A novel small-molecule MRCK inhibitor blocks cancer cell invasion. *Cell Commun. Signal.* 12:1–15, 2014.
- <sup>104</sup>Vennin, C., *et al.* Transient tissue priming via ROCK inhibition uncouples pancreatic cancer progression, sensitivity to chemotherapy, and metastasis. *Sci. Transl. Med.* 9:eaai8504, 2017.
- <sup>105</sup>Wang, Z.-M., D.-S. Yang, J. Liu, H.-B. Liu, M. Ye, and Y.-F. Zhang. ROCK inhibitor Y-27632 inhibits the growth, migration, and invasion of Tca8113 and CAL-27 cells in tongue squamous cell carcinoma. *Tumor Biol.* 37:3757–3764, 2016.
- <sup>106</sup>Wei, L., M. Surma, S. Shi, N. Lambert-Cheatham, and J. Shi. Novel insights into the roles of rho kinase in cancer. *Arch. Immunol. Ther. Exp. (Warsz)* 64:259–278, 2016.
- <sup>107</sup>Weng, S., Y. Shao, W. Chen, and J. Fu. Mechanosensitive subcellular rheostasis drives emergent single-cell mechanical homeostasis. *Nat. Mater.* 15:961–967, 2016.
- <sup>108</sup>Wirtz, D., K. Konstantopoulos, and P. C. Searson. The physics of cancer: the role of physical interactions and mechanical forces in metastasis. *Nat. Rev. Cancer* 11:512–522, 2011.
- <sup>109</sup>Wolf, K., *et al.* Physical limits of cell migration: control by ECM space and nuclear deformation and tuning by proteolysis and traction force. *J. Cell Biol.* 201:1069–1084, 2013.
- <sup>110</sup>Xiao, F., X. Wen, and P. Y. Chiou. Plasmonic micropillars for massively parallel precision cell force measurement. *Micro Electro Mech. Syst.* 1:243–246, 2017.
- <sup>111</sup>Xiao, F., X. Wen, X. H. M. Tan, and P.-Y. Chiou. Plasmonic micropillars for precision cell force measurement across a large field-of-view. *Appl. Phys. Lett.* 112:033701, 2018.
- <sup>112</sup>Xu, W., R. Mezencev, B. Kim, L. Wang, J. McDonald, and T. Sulchek. Cell stiffness is a biomarker of the metastatic potential of ovarian cancer cells. *PLoS ONE* 7:e46609, 2012.

- <sup>113</sup>Yachida, S., *et al.* Distant metastasis occurs late during the genetic evolution of pancreatic cancer. *Nature* 467:1114–1117, 2010.
- <sup>114</sup>Yamaguchi, H., and J. Condeelis. Regulation of the actin cytoskeleton in cancer cell migration and invasion. *Biochim. Biophys. Acta* 1773:642–652, 2007.
- <sup>115</sup>Ying, H., *et al.* The Rho kinase inhibitor fasudil inhibits tumor progression in human and rat tumor models. *Mol. Cancer Ther.* 5:2158–2164, 2006.
- <sup>116</sup>Yu, H. W., *et al.* PIX controls intracellular viscoelasticity to regulate lung cancer cell migration. *J. Cell Mol. Med.* 19:934–947, 2015.
- <sup>117</sup>Zaidel-Bar, R., G. Zhenhuan, and C. Luxenburg. The contractome—a systems view of actomyosin contractility in non-muscle cells. *J. Cell Sci.* 128:1–9, 2015.
- <sup>118</sup>Zhang, W., *et al.* Microfluidics separation reveals the stem-cell-like deformability of tumor-initiating cells. *Proc. Natl. Acad. Sci. USA* 109:18707–18712, 2012.
- <sup>119</sup>Zhao, S., Y. Wang, L. Cao, M. M. Ouellette, and J. W. Freeman. Expression of oncogenic K-ras and loss of Smad4 cooperate to induce the expression of EGFR and to promote invasion of immortalized human pancreas ductal cells. *Int. J. Cancer* 127:2076–2087, 2010.
- <sup>120</sup>Zhao, X., *et al.* Hypoxia-Inducible factor-1 promotes pancreatic ductal adenocarcinoma invasion and metastasis by activating transcription of the actin-Bundling protein fascin. *Cancer Res.* 74:2455–2464, 2014.
- <sup>121</sup>Zhou, L., *et al.* Theoretical modeling of mechanical homeostasis of a mammalian cell under gravity-directed vector. *Biomech. Model. Mechanobiol.* 17:191–203, 2018.
- <sup>122</sup>Zhu, F., *et al.* Rho kinase inhibitor fasudil suppresses migration and invasion through down-regulating the expression of VEGF in lung cancer cell line A549. *Med. Oncol.* 28:565–571, 2011.

**Publisher's Note** Springer Nature remains neutral with regard to jurisdictional claims in published maps and institutional affiliations.